Tectonics

Supporting Information for

Strike-slip Enables Subduction Initiation beneath a Failed Rift: New Seismic Constraints from Puysegur Margin, New Zealand

Brandon Shuck[1,2], Harm Van Avendonk[1], Sean P. S. Gulick[1,2], Michael Gurnis[3], Rupert Sutherland[4], Joann Stock[3], Jiten Patel[4], Erin Hightower[3], Steffen Saustrup[1], Thomas Hess[1,2]

[1]Institute for Geophysics, Jackson School of Geosciences, University of Texas at Austin, Austin, TX 78758, USA.
[2]Department of Geological Sciences, Jackson School of Geosciences, University of Texas at Austin, Austin, TX 78712
[3]Seismological Laboratory, California Institute of Technology, Pasadena, CA 91125, USA.
[4]School of Geography, Environment and Earth Sciences, Victoria University of Wellington, Wellington 6140, New Zealand.

Corresponding author: Brandon Shuck (brandon.shuck@utexas.edu)

Contents of this file

Introduction

This supporting document includes text and figures for the article: Strike-slip Enables Subduction Initiation beneath a Failed Rift: New Seismic Constraints from Puysegur Margin, New Zealand. Text S1 contains detailed information about the SISIE marine geophysical survey and data acquisition. Text S2 contains information about post-cruise OBS data processing. Text S3 describes the interpretation of OBS records and the tomographic inversion process. Text S4 contains a description of the MCS data processing workflow. Figure S1 presents crustal stretching factors and extension calculations for the Solander Basin rift domain on the SISIE-1 and SISIE-2 profiles. Figure S2 illustrates updated correlations of chronostratigraphic horizons from Patel et al. (2020) and tectonostratigraphic packages

interpreted in this study, which are aligned with the New Zealand (Raine et al., 2015) and international Geologic Time Scale (Gradstein et al., 2012). Figure S3 through Figure S7 are show comparisons between the uninterpreted and interpreted seismic sections shown in the main article.

Text S1

South Island Subduction Initiation Experiment (SISIE) Data Acquisition

The South Island Subduction Initiation Experiment (SISIE) took place in February and March, 2018. Using the R/V *Marcus Langseth*, the shipboard party collected multichannel seismic (MCS), ocean-bottom seismometer (OBS), 2-6 kHz chirp, 12 kHz multi-beam bathymetry, gravity, and magnetometer data across the Puysegur margin. For seismic imaging, the acoustic source consisted of an array of 36 Bolt airguns, with a total source volume of ~6600 in^3, shot at intervals of 50 m for MCS and 150 m for OBS acquisition. A 12.6 km hydrophone streamer containing 1008 channels was used to collect an initial 717 km of MCS data (SISIE-1, SISIE-2, SISIE-3, SISIE-4, SISIE-5); however, severe weather of up to 7 meter swells forced the collection of the remaining 535 km to be with a 4.05 km streamer containing 324 channels (SISIE-6 and SISIE-8). In total, 1252 km of MCS data were acquired along seven 2D lines. Short-period four-component OBSs from the University of Texas Institute for Geophysics were used for a total of 43 deployments spaced approximately 15 km apart on two east-west oriented transects, SISIE-1 and SISIE-2. Seismic data were successfully recovered from 39 of these instruments. More details of the marine expedition can be found in the MGL1803 cruise report: http://www.marine-geo.org/link/data/field/Langseth/MGL1803/docs/MGL1803_DataReport_Ver1.1.pdf. Raw and processed geophysical data from cruise MGL1803 are available from the Marine Geoscience Data System http://www.marine-geo.org/tools/search/entry.php?id=MGL1803.

Text S2

Ocean Bottom Seismometer Data Processing

Following recovery of the OBSs, a GPS clock synchronization corrected for clock drift, and seismic data were cut into 60-second-long records and then converted to SEG-Y format. The OBS data are generally high quality and show distinct seismic reflections and refractions

from the crust and mantle on most instruments. To enhance the clarity of these arrivals, a bandpass filter of 6-14 Hz with 48 dB/octave drop-off was applied. A predictive deconvolution filter with a 160 ms gap was applied to help enhance the refracted arrivals. The hydrophone channel has higher signal/noise ratio than the vertical and horizontal geophone channels, and thus was used for a majority of the OBS data interpretation. To ensure accurate source-receiver offsets, the precise location of all instruments on the seafloor were determined using direct water-wave arrivals.

Text S3

OBS Tomographic Inversion and Model Resolution Test

Distinct wide-angle seismic phases including crustal refractions (Pg), Moho reflections (PmP) and mantle refractions (Pn) were identified on OBS records on the SISIE-1 and SISIE-2 profiles. The OBS data are high quality allowing for clear interpretation of these phases throughout most instruments along the two profiles. Assigned picking errors were typically between 50-200 ms. Tomographic inversion of all travel-time data was performed using the approach described by Van Avendonk et al. (2004). An initial first arrival tomography model was used as a starting point for a more advanced layered model. Layers were then inserted for the sediments, crust, and mantle. The seafloor boundary was extracted from the NIWA bathymetry grid. The boundary between the sediments and crust were guided by coincident MCS images. A top-down approach was taken by first raytracing and inverting shallow phases and progressively adding in deeper phases. This process was repeated iteratively and simultaneously constrained layer boundaries and seismic velocities. The models were updated until the travel-time misfit was similar to the average uncertainty of picked phases. The final result yields a smooth characterization of the seismic velocity structure along the two profiles. The robustness of the tomography models was evaluated using a standard resolution test. We tested the recovery of a 12 km horizontal by 6 km vertical perturbation ellipse. Resolution of seismic velocities and model layer boundaries are shown in Figure 4.

Text S4

Multichannel Seismic Reflection Data Processing

Seismic processing of the SISIE MCS data utilized the Echos and Geodepth software packages from Emerson/Paradigm Geophysical. First, the SEGD traces were input into Echos and resampled to 4 ms. Noise reduction consisted of trace editing to remove noisy channels and bandpass filtering (7-85 Hz). Interpolation was applied first to shot gathers to fill in missing channels, and then in the receiver domain to recover signal from low-energy shots recorded during marine mammal shutdowns. We used a marine 2-D geometry of 50 m shot spacing and 12.5 m receiver group spacing. Semblance-based velocity analysis was performed approximately every 500 CMPs (~3 km). Multiple suppression comprised a combination of surface-related multiple elimination (SRME) in the shot domain followed by parabolic radon transforms in the CMP domain, and finally a dip filter to remove undercorrected multiple arrivals and out-of-plane energy. Velocity models for Kirchhoff pre-stack depth migration algorithms were derived from the RMS stacking velocities. For MCS lines coincident with OBS data, a merged velocity section with MCS-derived velocities for shallow sediments and OBS-derived velocities for crust and mantle structure produced the best images. Kirchoff pre-stack depth migrations were performed using an Eikonal travel-time fitting algorithm with a migration aperture of 2000 or 4000 CMPs. Velocity models were iteratively updated until the final depth-migrated image gathers were flattened. Outside muting removed stretched reflections at far offsets and inside muting removed residual multiple energy. The depth-migrated gathers were bandpass filtered, mixed with 3 adjacent traces, and then stacked. The result of our processing workflow yields seven pre-stack depth migrated (PSDM) lines across the Puysegur margin.

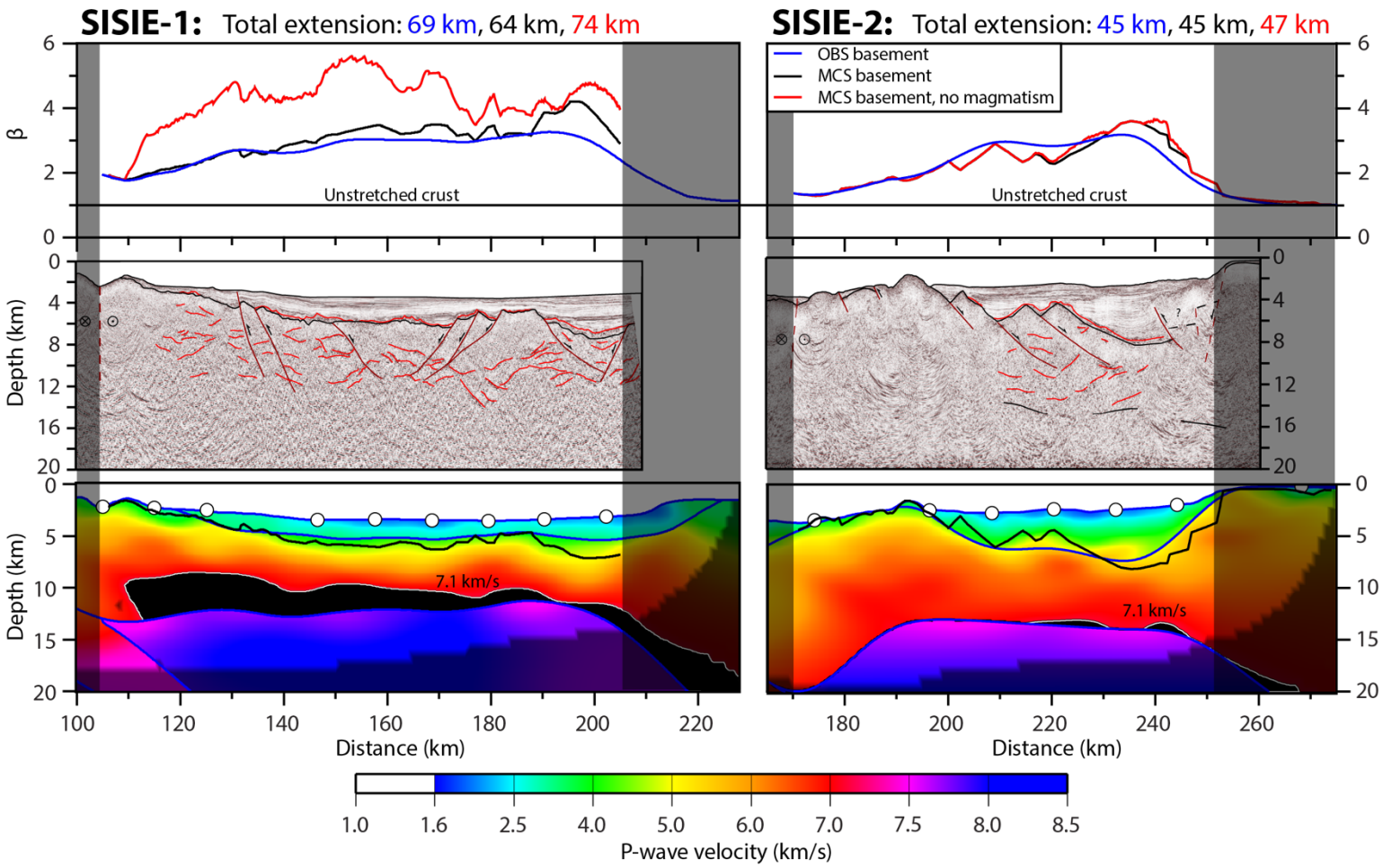

Figure S1. Analysis of the Solander Basin rifted margin domains along the SISIE-1 (left) and SISIE-2 (right) profiles. Shaded areas represent either the western boundary of the rifted margin domain or the loss of Moho resolution beneath the Campbell Plateau. Crustal thickness was calculated in two ways: (1) using the top of basement and Moho constrained by the tomographic models, and (2) using the basement from the MCS image and Moho from the tomographic models. Crustal stretching factors were then calculated by dividing the initial crustal thickness of 21 km (Grobys et al., 2008) by the present-day crustal thickness. Stretching was assumed to be isotropic with depth, resulting in a 1D β-factor distribution across the rifted margin domain. The amount of total extension was calculated by integrating the β-factor over the same domain.

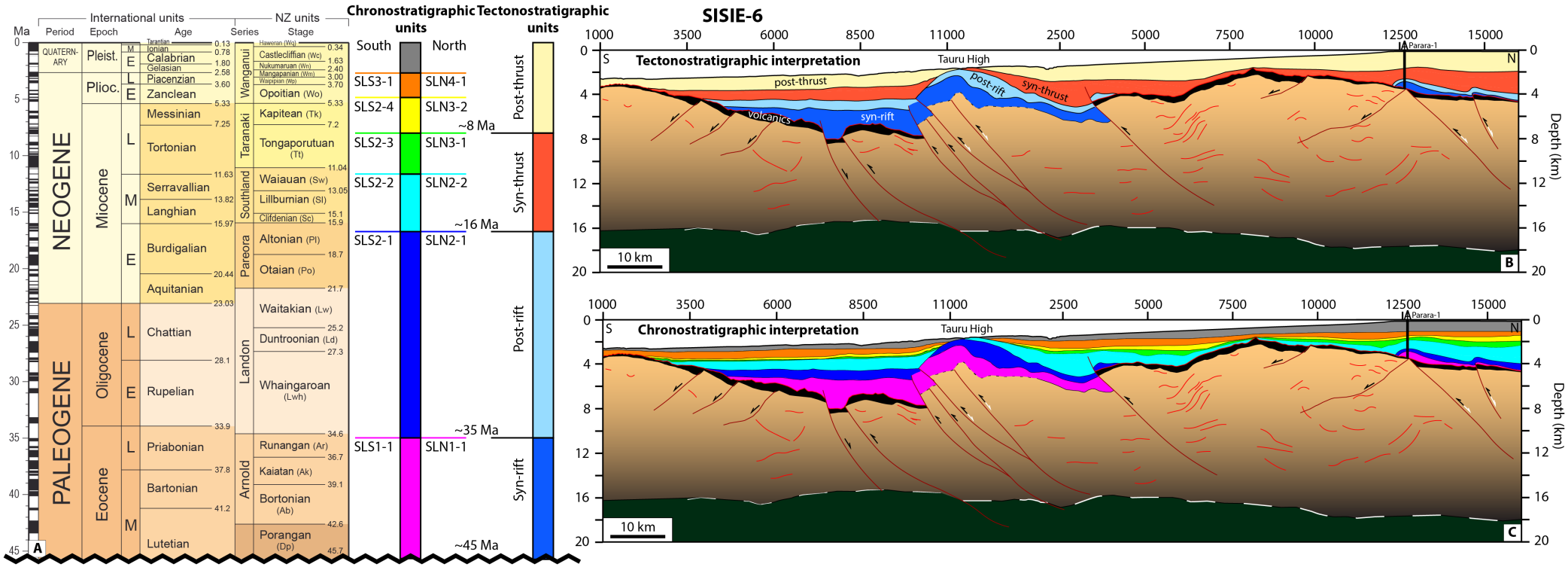

Figure S2. Chrono- and tectonostratigraphic interpretations of the SISIE-6 profile. The upper boundaries of SLS1-1 and SLN1-1 on the seismic image have been revised after Patel et al. (2020). Correlations across the Tauru Fault Zone are based on similar thickness, seismic character, and onlap relationships of respective units. New Zealand Geologic Time scale modified from Raine et al. (2015).

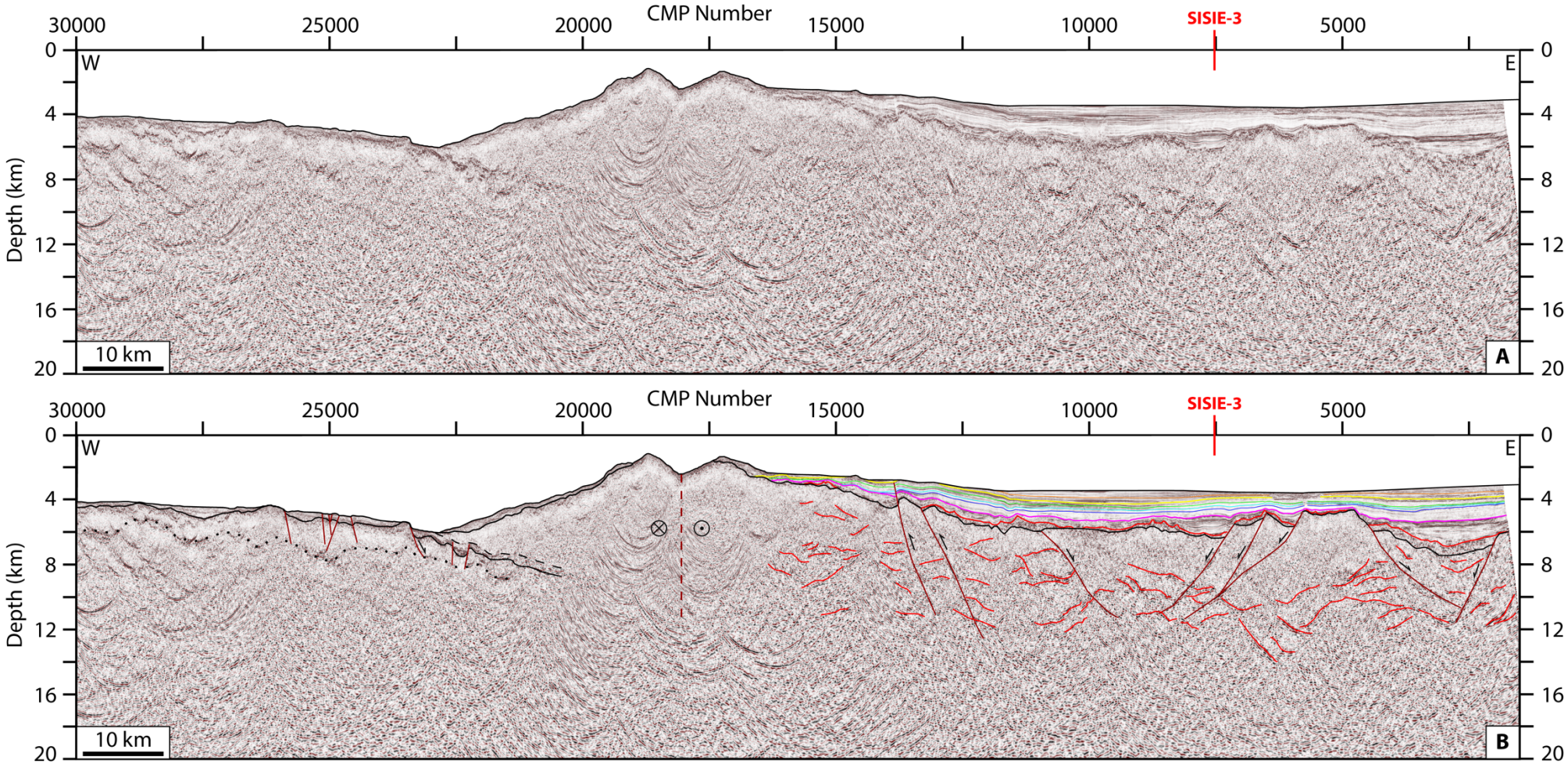

Figure S3. Uninterpreted (top) and interpreted (bottom) pre-stack depth migrated seismic image of the SISIE-1 profile.

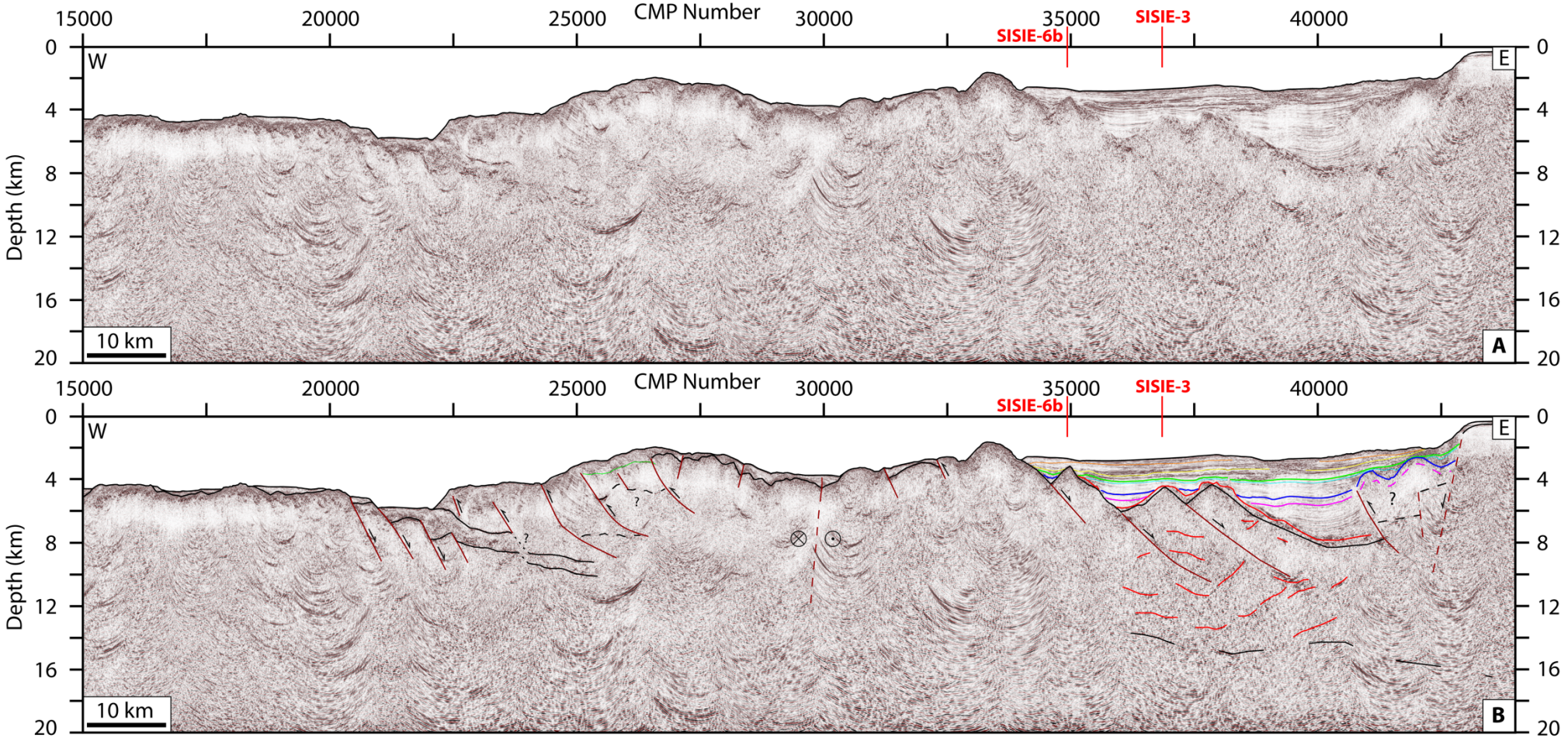

Figure S4. Uninterpreted (top) and interpreted (bottom) pre-stack depth migrated seismic image of the SISIE-2 profile.

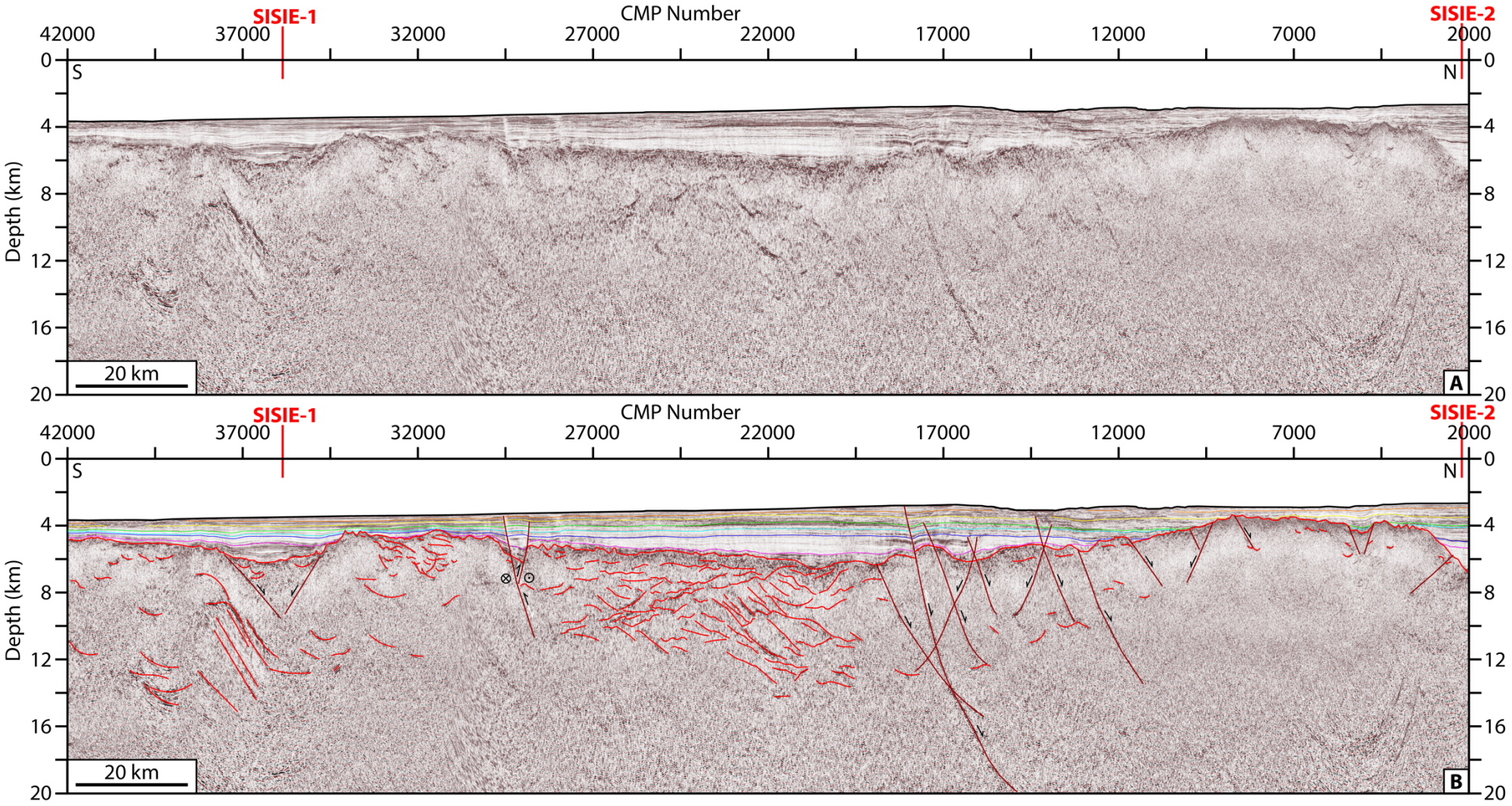

Figure S5. Uninterpreted (top) and interpreted (bottom) pre-stack depth migrated seismic image of the SISIE-3 profile.

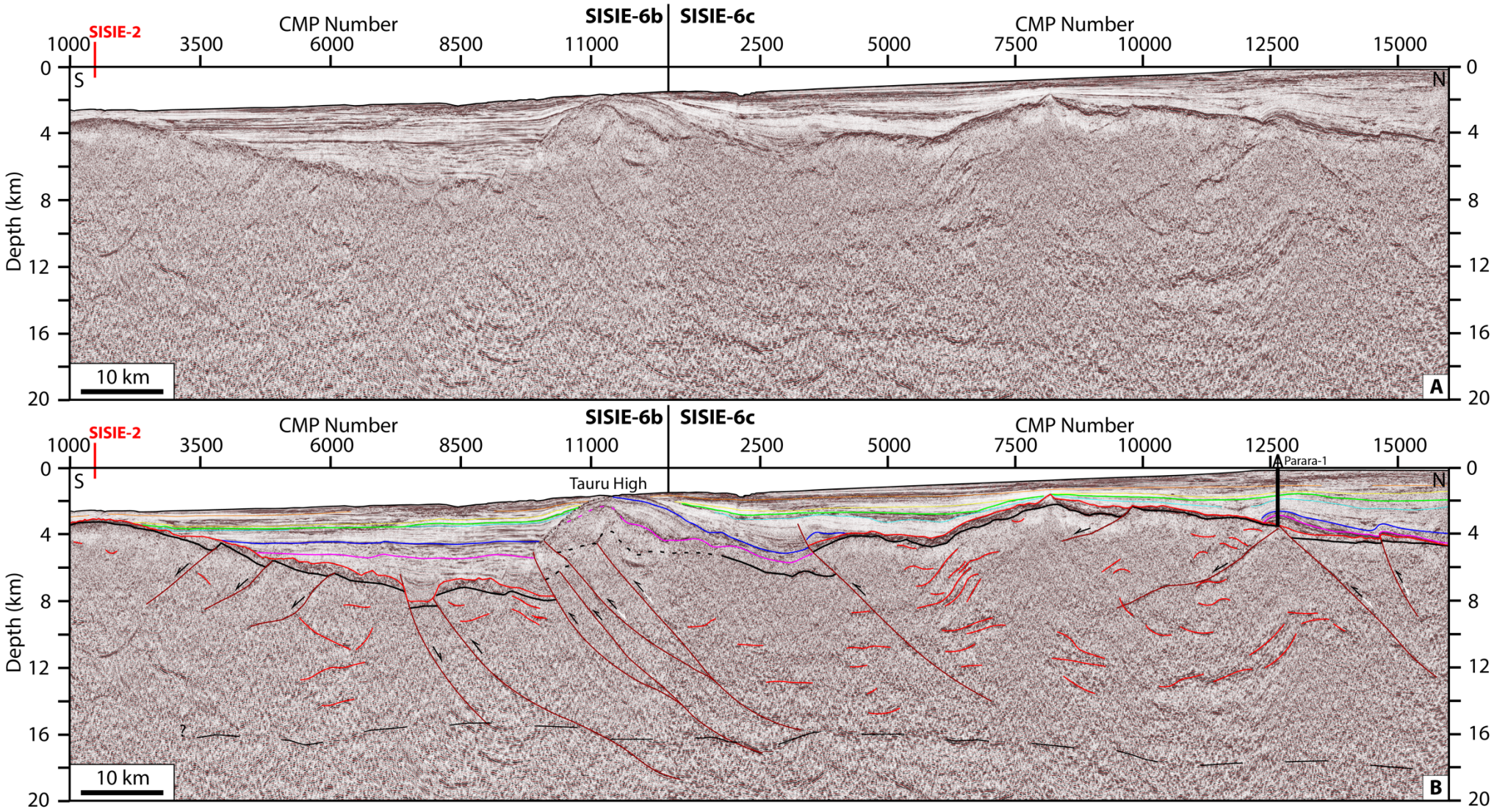

Figure S6. Uninterpreted (top) and interpreted (bottom) pre-stack depth migrated seismic image of the SISIE-6 profile.

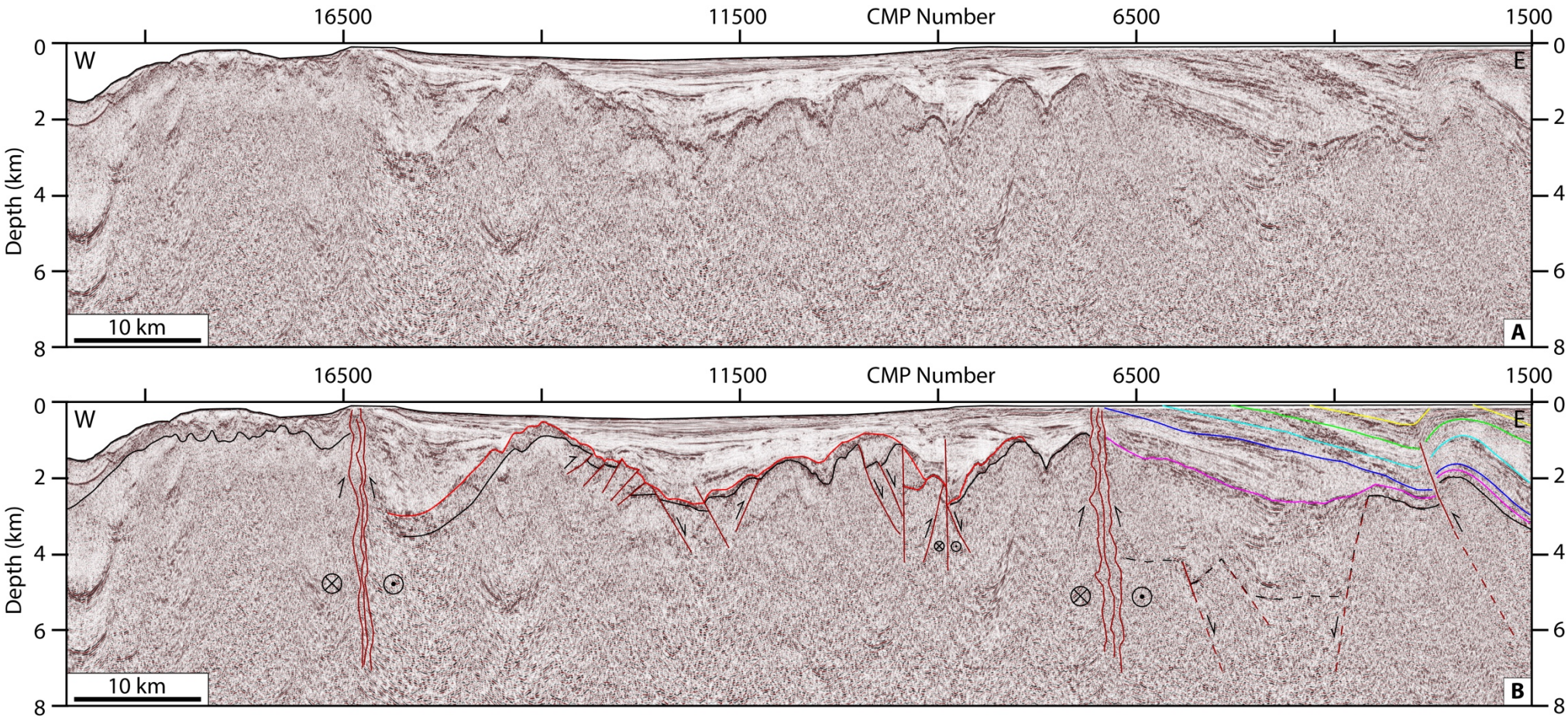

Figure S7. Uninterpreted (top) and interpreted (bottom) pre-stack depth migrated seismic image of the SISIE-8 profile.